Complex Rheological Properties of a Water-Soluble Extract from the Fronds of the Black Tree Fern, *Cyathea medullaris*

Kelvin K. T. Goh,*,† Lara Matia-Merino,† Christopher E. Hall,† Paul J. Moughan,‡ and Harjinder Singh‡

Institute of Food, Nutrition and Human Health, and Riddet Centre, Massey University, Private Bag 11 222, Palmerston North, New Zealand

Received May 15, 2007; Revised Manuscript Received August 17, 2007

A water-soluble extract was obtained from the fronds of a New Zealand native black tree fern (*Cyathea medullaris* or Mamaku in Māori). The extract exhibited complex rheological behavior. Newtonian, shear-thinning, shear-thickening, thixotropic, antithixotropic, and viscoelastic behaviors were observed depending on polymer concentration, shear rate, and shear history. The extract also displayed rod-climbing and self-siphoning properties typical of viscoelastic fluids. Such complex rheological properties have been reported in synthetic or chemically modified polymers but are less frequent in unmodified biopolymers. Although Mamaku extract obtained from the pith of the fern has been traditionally used by the Māori in New Zealand for treating wounds and diarrhea among other ailments, this material has never been characterized before. This study reports on the chemical composition of the extract and on its viscoelastic properties through rotational and oscillatory rheological measurements. Explanations of the mechanism behind the rheological properties were based on transient network models for associating polymers.

1. Introduction

The black tree fern (*Cyathea medullaris*), known as "Mamaku" in Māori, is the tallest tree fern found throughout the South Pacific. Traditionally, the pith of the trunk and fronds were consumed by natives and early explorers. The cooked pith was described as soft with a very sweet taste.[1] The uncooked pith is slimy due to the presence of a brownish-red mucus-like fluid. The mucus-like material was also used traditionally for various medicinal purposes such as treating wounds and boils,[2] as a vermifuge, and as a remedy for diarrhoea.[2] The functions of mucus-like sap found in the trunk and fronds of Mamaku are not well-established. To our current knowledge, this mucus-like material has not been characterized. In this first paper, we report on the isolation and unusual rheological properties of the water-soluble extract.

Rheological measurements based on steady shear, oscillatory shear, and step strain experiments have been used to characterize the viscous and elastic properties of fluids. The physical manifestation of the elastic component in viscoelastic fluid behavior is commonly demonstrated by "the tubeless siphon", "die swell", or "rod-climbing" effects. It is well-established that these effects are the result of the development of normal stresses within the fluid that overcome centrifugal or gravitational forces.[3] The elasticity in polymer solutions has been related to a shear-thickening behavior that corresponds well to the first normal stress coefficient under shear.[4]

Under flow, shear-thickening behaviors are rare in many biopolymer solutions. However, they are known to occur in complex fluids such as dense suspension,[5] wormlike micelles, and associating polymer solutions.[6,7] Associating polymers are polymers that contain functional groups along polymer chains that are capable of interacting with each other in a selective solvent.[8] Reversible cross-links which can be formed at the junctions are usually due to noncovalent interactions such as hydrophobic and hydrogen bonds. Disruption and reformation of molecular networks at the junctions can occur due to conditions such as an increase in temperature and/or application of stresses. Such physical networks are defined as transient networks.[9] A common example of associating polymers is the telechelic polymers (polymer molecules carrying associative end groups). The rheological properties of these polymers often exhibit Newtonian behavior at low shear rates, shear-thickening behavior at intermediate shear rates, and then shear-thinning at higher shear rates.[4] Shear-thickening behavior in associating polymer solutions has been a subject of research since the 1950s.[8]

Other systems that reported shear-thickening include interpolyelectrolyte systems,[10] shear-induced formation of intermolecular aggregates in spider silk dope,[11] soluble starch solutions,[12,13] and in a low-methoxy pectin solution.[14] Shear-thickening behavior seems to be identical for many systems from a rheological viewpoint. However, the molecular origin of the complex formation may differ (e.g., electrostatic interaction, hydrogen bonding, cross-linking by crystalline segments, and coordination with metallic ions, among others), depending on each system.[15] In this paper, we report on the shear-thickening behavior of the solutions prepared from a freeze-dried crude water-soluble extract of the fronds of Mamaku.

2. Materials and Methods

2.1. Isolation of Mamaku Extract. The fronds of the tree fern were obtained from the Massey University campus in Palmerston North, New Zealand during the month of January 2006. The leaves on the fronds were removed, and the fronds were washed and cut into slices of approximately 5 mm thick using a slicer (Dito-Sama, Aubusson, France). Warm water (~50 °C) was added to the sliced fronds in

* Corresponding author. E-mail: K.T.Goh@massey.ac.nz. Tel.: 64-6-3504366, ext 7195. Fax: 64-6-3505657.
† Institute of Food, Nutrition and Human Health.
‡ Riddet Centre.

10.1021/bm7005328 CCC: $37.00
Published on Web 10/16/2007

roughly equal proportion. The mixture of sliced fronds was blended in a wet disintegrator (Jeffco, Dry Creek, Australia) for 5 min. This step removed the mucus-like material from the fronds into the continuous phase of the mixture. The crude water-soluble extract was separated from the disintegrated fronds using muslin cloth. The crude extract solution was then centrifuged at 13 600*g* for 30 min at 20 °C (RC5C Sorvall centrifuge and GS-3 rotor, Kendro Laboratory Products GmbH, Langenselbold, Denmark) to remove any insoluble materials. The supernatant was then freeze-dried. This extraction method yields approximately 1% (w/w) of freeze-dried material.

2.2. Chemical Analysis. Elemental analyses for C, H, N, O on the freeze-dried sample were carried out using a Carlo Erba elemental analyzer EA 1108 (Carlo Erba Instruments, Milan, Italy) by the Campbell MicroAnalysis Laboratory, University of Otago, New Zealand. Mineral composition was determined using inductively coupled plasma−optical emission spectrometer by accredited AgriQuality Laboratory, Auckland, New Zealand. Proteins, total lipid, ash, and condensed tannins (%) were determined by an accredited chemical laboratory (accredited Nutritional Laboratory, Institute of Food, Nutrition & Human Health, Massey University) based on AOAC 991.36, AOAC 968.06, AOAC 942.05, and AOAC 962.09 and HCL−butanol methods, respectively. The percent total sugar was determined using the phenol−sulfuric acid method.[16] Nonstarch polysaccharide was determined using the Englyst method,[17] neutral sugars were analyzed by gas chromatography, and the uronic acid was determined by a spectophotometric method.[18]

2.3. Rheological Measurements. Freeze-dried Mamaku extracts (2%, 4%, 6%, 8%, and 10%, w/w) were redispersed in 0.1 M NaCl solutions containing 0.02% (w/w) sodium azide. The samples were allowed to hydrate for ~24 h at 20 °C and centrifuged at 3100*g* for 30 min at 20 °C (Centra MP4R and Rotor 224, International Equipment Company, Needham Heights, MA). Rheological measurements were performed in both oscillatory and rotational (steady-state flow) modes using the Paar Physica rheometer MCR 301 (Anton-Paar, Graz, Austria). The rheometer was equipped with a cone and plate geometry (CP 40-4 and P-PTD200/56, gap = 0.049 μm) or a double-gap measuring system (DG 26-7 and C-PTD 200). The rheometer has a Peltier element to control temperature using the computer software, Rheoplus v2.65. All measurements were made at 20 ± 0.1 °C. A dynamic oscillatory stress sweep test was first performed at a frequency of 1 Hz to determine the linear viscoelastic region for all samples using the double-gap measuring system. The strain value obtained within the linear viscoelastic region (5%) was used in performing frequency sweep tests (30 data points, 0.01−100 Hz). In rotational mode, viscosity flow curves and the first normal stress difference (N_1) curves were initially obtained using the cone and plate measuring system. The first normal stress difference is defined as

$$N_1 = \frac{2F}{\pi R^2} \tag{1.1}$$

where F is the normal force; R is the radius of the cone−plate geometry.[19] Another way to describe first normal stress difference is based on the Rouse model as recently described by Tuinier et al.[20] and is expressed as

$$N_1 = \dot{\gamma}\,\frac{36}{\pi^4}\,\frac{(\eta_0 - \eta_s)^2 M}{RTc} \tag{1.2}$$

where $\dot{\gamma}$ is the shear rate, η_0 is the zero shear rate viscosity, η_s is the viscosity of the solvent, M is the molar mass of the EPS molecule, R is the gas constant, T is the temperature, and c is the polymer concentration.

The sweep-up and sweep-down viscosity measurements for solutions of different polymer concentrations were also carried out using a double-gap measuring system (30 data points, 0.001−1000 s^{-1}). Furthermore, viscosity measurements were performed at constant shear rates (0.1, 1, 10, and 100 s^{-1}), each for the duration of 1000 s. To ensure that all rheological data were valid, values obtained below the minimum detectable torque of 0.02 (μNm) were discarded. All measurements were carried out in replicate.

Table 1. Composition of Freeze-Dried Mamaku Extract

composition	% (w/w)
moisture	9.25
ash	16.07
crude protein	2.02
fat	0.17
crude fiber	0.24
tannins	0.09
sugars	44.3
nonstarch polysaccharides	9.80
unknown	18.06
minerals	**(mg/kg)**
potassium	51800
sodium	30400
calcium	1200
magnesium	1000
aluminum	710
zinc	54
manganese	26
iron	7.7
copper	7.4
selenium	0.28
lead	0.072
mercury	<0.01

The viscosities of dilute Mamaku solutions (<1% w/w) were determined using a Cannon−Ubbelohde low shear four-bulb capillary viscometer (viscometer no. 75, S766, Cannon Instrument Co., PA). The relative viscosity (η_{rel}) of the sample was obtained at 20 °C according to

$$\eta_{rel} = \frac{t\rho}{t_s\rho_s} \tag{1.3}$$

where t and t_s are the efflux times for the Mamaku solutions and solvent, respectively; ρ and ρ_s are the densities of the solution and solvent, respectively.

From the η_{rel}, the specific viscosity (η_{sp}) is obtained by

$$\eta_{sp} = \eta_{rel} - 1 \tag{1.4}$$

3. Results and Discussion

3.1. Chemical Analysis. Elemental analysis (C, H, N, O) of freeze-dried extract shows that it consisted of 32.78% C, 5.53% H, 0.37% N, and 52% O. This gives an approximate empirical formula of $C_6H_{12}O_7$. The mineral composition and the contents of several other chemical entities are given in Table 1. The water-soluble extract consisted of a large proportion of sugar (~44%), ~10% nonstarch polysaccharides (NSP), and a low amount of proteins (~2%). The NSP fraction consisted of uronic acid (72.5%), galactose (14.3%), xylose (7.1%), and arabinose (3.1%). Small quantities of other monosaccharides present were rhamnose (~1%), fucose (~1%), mannose (~1%), and glucose (<1%). The crude extract had a relatively high mineral content (~16%). The extract seems to be especially rich in potassium, sodium, calcium, magnesium, and aluminum. From the chemical analysis, a residual ~18% of the extract freeze-dried matter remains unidentified.

3.2. Visual Observation of Viscoelastic Properties. A semidilute solution of Mamaku extract (7% w/w) prepared by

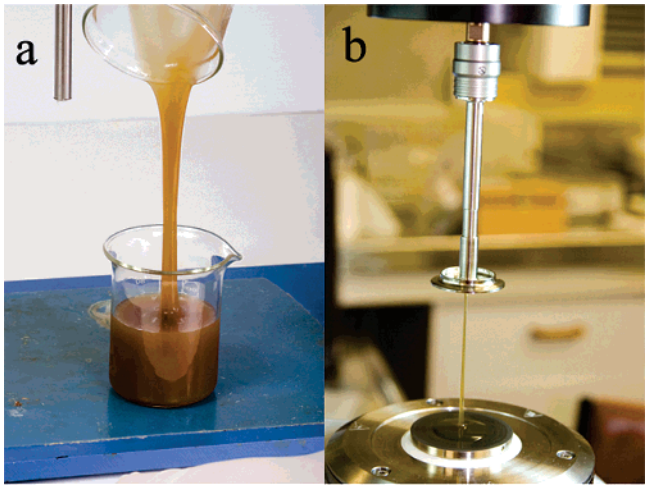

Figure 1. Viscoelastic properties of 7% w/w solution of Mamaku extract illustrated by (a) decanting from one beaker to another and (b) lifting the cone geometry from the plate after performing a viscosity measurement.

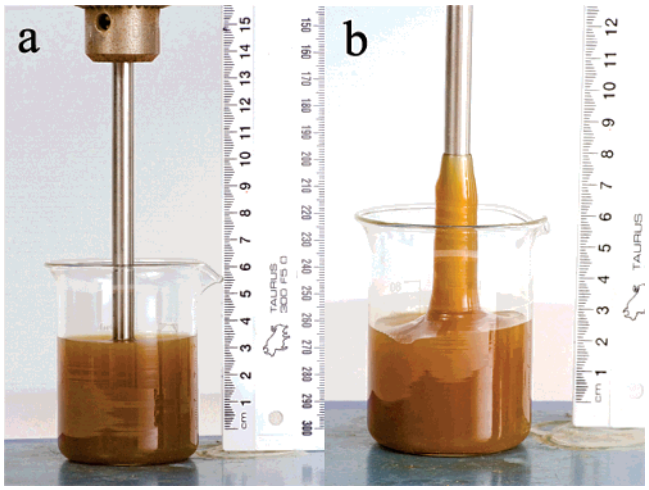

Figure 2. (a) 7% w/w solution of Mamaku extract with the rod (6 mm diameter) stationary. (b) Rod-climbing effect of the same solution when the rod (8 mm diameter) was rotated at ~120 rev/min.

dispersing freeze-dried extract in Milli-Q water containing 0.1 M NaCl and 0.02% (w/w) sodium azide exhibited interesting viscoelastic properties. When the solution of Mamaku extract was poured from a beaker (Figure 1a) or when the cone geometry was lifted after a rheological measurement (Figure 1b) the fluid showed interesting elastic behavior. The solution was able to "stretch" for a reasonable distance (~25 cm) until the gravitational force overcame its elastic character.

The solution was also found to exhibit rod-climbing ability (Figure 2a and 2b) and self-siphoning effect (figure not shown). The rod-climbing effect (also known as Weissenberg effect) has been observed in some polymer melts and crude oils[21,22] but rarely observed in natural polymers. The rod-climbing ability of the solution suggests that the shear may stretch and orient the polymer molecules creating normal stresses. The anisotropy induced is such that the fluid is pulled inward and climbs the rod.[3]

The interesting rheological behavior of the Mamaku extract was likely to be due to the presence of large macromolecular species present. On the basis of the chemical composition of the water extract (Table 1), these polymer molecules are probably the nonstarch polysaccharide fraction present at ~10% w/w of the freeze-dried extract. Further work is underway to purify and characterize this fraction.

3.3. Rheological Characterization. Rheological measurements were performed to quantify the viscous and elastic characteristics of the rehydrated freeze-dried extract. Steady-state viscosity measurements were carried out using the solutions of the Mamaku extract (2%, 4%, 6%, 8%, and 10% w/w) dispersed in Milli-Q water containing 0.1 M NaCl and 0.02% sodium azide. These solutions are equivalent to ~0.2%, 0.4%, 0.6%, 0.8%, and 1% w/w the nonstarch polysaccharide fraction. The viscosity flow curves (Figure 3) exhibited a region of Newtonian behavior at low shear rates, followed by a shear-thickening region at intermediate shear rates, and then a shear-thinning region at higher shear rates. The Newtonian region was apparent for solutions at higher concentration (at 1 s^{-1} for 10% w/w Mamaku), but as the polymer concentration was decreased, the Newtonian region could not be measured due to the limited sensitivity of the rheometer. As the polymer concentration decreased, the onset of shear-thickening was also shifted to higher shear rates (from 4 s^{-1} at 10% w/w solution to 30 s^{-1} at 4% w/w solution). At 2% w/w Mamaku solution, the effect of shear-thickening diminishes and the viscosity curve approaches Newtonian behavior.

Data on the first normal stress difference (N_1) were also obtained during the viscosity measurements using the cone and plate geometry (Figure 3). The first normal stress difference is traditionally used to measure the viscoelastic quantities often defined by processes like rod climbing or the Weissenberg effect. It is therefore not surprising that positive N_1 values were observed for semidilute Mamaku solutions. The increase in N_1 within a certain shear rate appears to correspond to the entire shear-thickening region of the viscosity curve with highest values of N_1 and η_{app} occurring at the same shear rate for each concentration of the Mamaku solution. As N_1 indicates the degree of elasticity of the Mamaku solution during shear, it implies that the onset of shear-thickening was the result of an increased elastic property in the polymer system during shear. The presence of normal stress in fluids may be exploited, for example, to provide load bearing between the parallel faces of a mechanical face seal or a plain thrust bearing.[23]

It was also observed that, before the onset of shear-thickening, the samples were seen to be dragged around as the cone rotated. However, no sample was lost during the entire run. Such flow instability has been reported for some telechelic polymers[24] and liquid crystalline solutions[25] at relatively low shear rates. It has been suggested that if only part of the sample remains in contact with the cone and plate and the actual area of contact is unknown, then correct data of the true rheological properties cannot be valid in this regime. According to Kosvintsev et al.,[26] it is not possible to conclude whether the changes observed should be regarded as a kind of shear-induced phase transition or merely as a mechanical instability. Hence, in order to verify that the measurement was reliable, the double-gap geometry was used instead since the sample would have a better chance to remain in the cup during the shearing process. Similar results were obtained (Figure 5) confirming that the shear-thickening property is likely to have a molecular origin, being independent of the geometry used. All subsequent rheological measurements were carried out using the double-gap geometry.

Frequency sweeps at 5% strain—within the linear viscoelastic region—were carried out for the Mamaku solutions at the same concentrations as above (4%, 6%, 8%, and 10% w/w). Samples containing 6%, 8%, and 10% Mamaku extract showed viscoelastic behavior within the frequency range of 0.01−10 Hz.

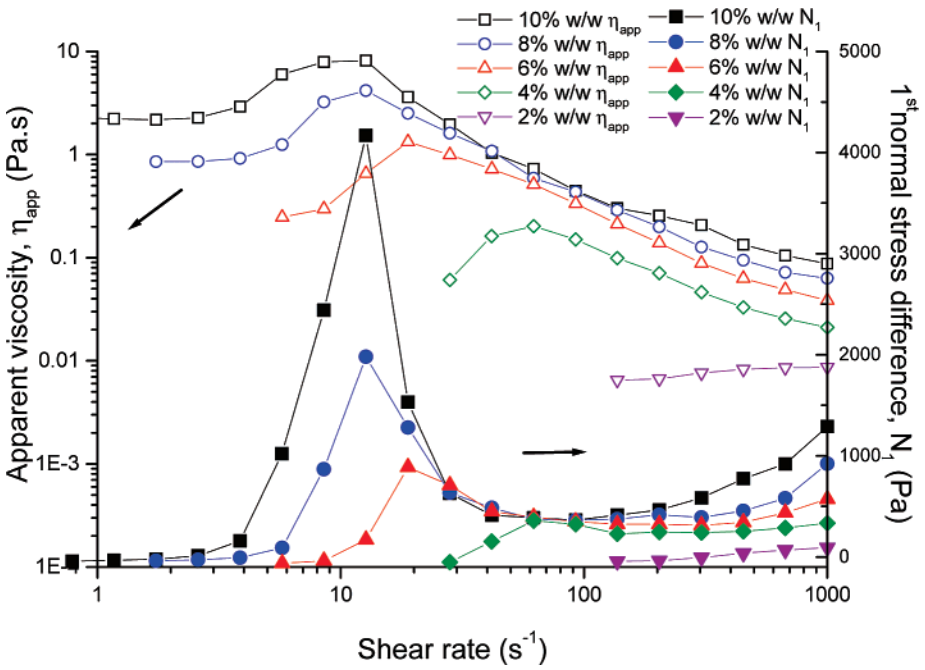

Figure 3. Apparent viscosity and first normal stress difference profiles of 2%, 4%, 6%, 8%, and 10% w/w Mamaku solutions as a function of shear rate, at 20 °C and using a cone and plate geometry.

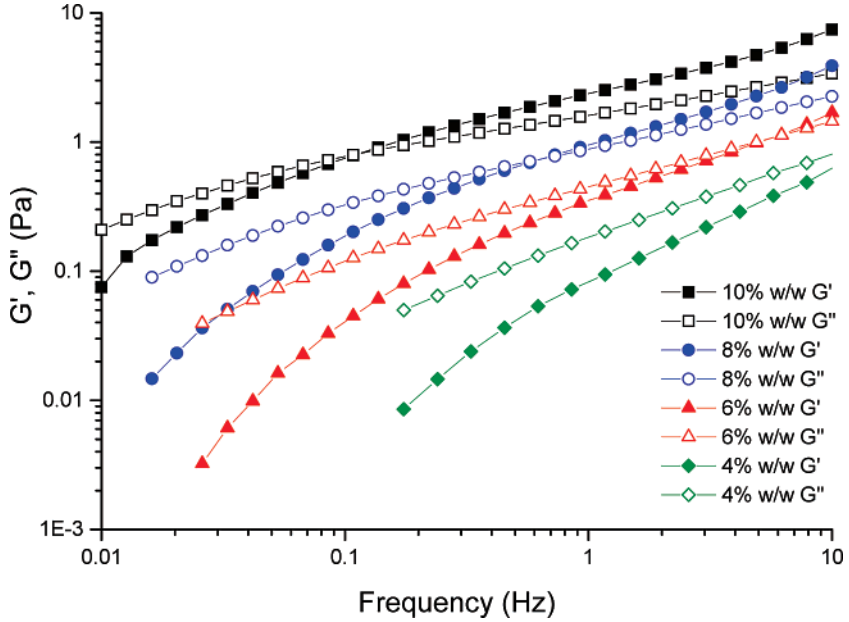

Figure 4. Elastic modulus (G', filled symbols) and viscous modulus (G'', open symbols) of the solutions of Mamaku extract (4%, 6%, 8%, and 10% w/w) plotted as a function of frequency obtained by oscillatory measurement. The mechanical spectra were obtained using a double-gap attachment.

As seen in Figure 4, the viscous modulus (G'') is above G' (elastic modulus) at low frequencies but G' dominated over G'' above the crossover frequency ($G' = G''$). The crossover point for each solution is shifted to higher frequencies as the concentration of the extract decreases, as expected in typical polymer solutions.[27] This implies that the relaxation time increases with increasing polymer concentration, reflecting an increase in the size and/or number of cross-linking points polymer chains. At 4% w/w Mamaku solution, the viscous modulus (G'') dominated throughout the entire frequency range.

As mentioned earlier, viscosity measurements obtained by using the double-gap geometry (Figure 5) were similar to those obtained by cone and plate geometry (Figure 3). Additional data points were obtained at lower shear rates due to the larger surface area of the double-gap geometry (Figure 5). It was again observed that just before the onset of shear-thickening at shear rates greater than ~3 s^{-1}, a small portion of the sample appeared to "climb" out of the gap between the rotating bob and the cup. However, the effect (i.e., samples coming out of the gap) was less pronounced than with the cone and plate geometry. It is unlikely that the viscosity values obtained in the shear-thickening region are affected by the small amount of sample coming out of the gap (given the large contact area of the double-gap geometry).

Figure 5 also shows complex viscosity (η^*) curves (obtained from oscillatory measurements) as a function of angular

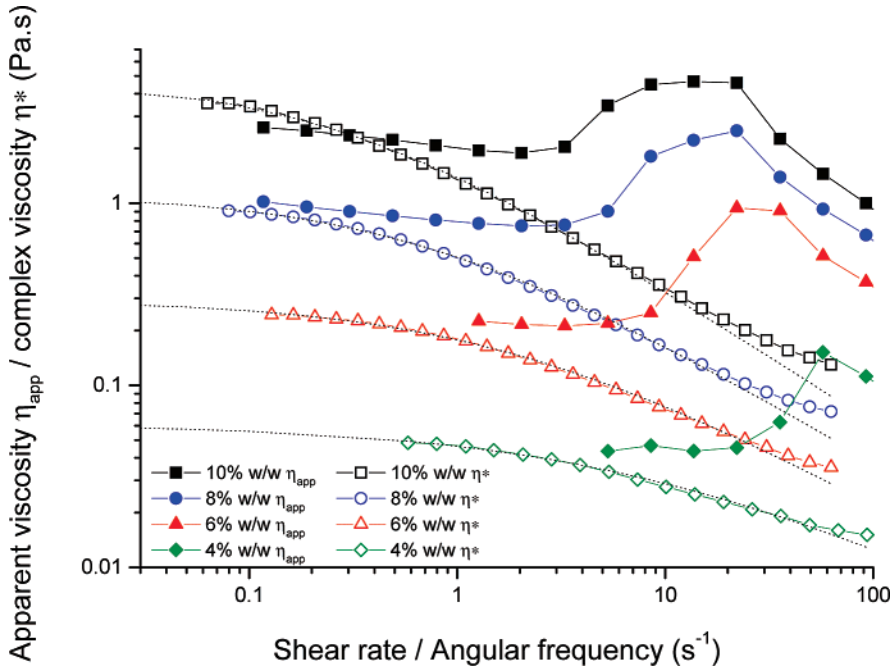

Figure 5. Superposition of apparent viscosity (η_{app}, filled symbols) obtained by rotational measurements and complex viscosity (η^*, open symbols) obtained by oscillatory measurements at 20 °C and as a function of shear rate and angular frequency, respectively, for Mamaku solutions (4%, 6%, 8%, and 10% w/w). Dotted lines show fits by the Cross equation.

frequency together with the viscosity curves (η_{app}) as a function of shear rate ($\dot{\gamma}$). The complex viscosity is defined by

$$\eta^* = \sqrt{(G')^2 + (G'')^2}/\omega$$

where G' is the elastic modulus and G'' is the viscous modulus.

Figure 5 clearly showed that the Cox−Merz rule fails for this type of rheological behavior. The Cox−Merz rule asserts that $|\eta^*(\omega)| = \eta(\dot{\gamma})$ for fluids that can be disrupted by large strain.[28] The longest relaxation time from frequency sweep ($G' = G''$) does not coincide at all with the onset of shear-thinning which occurs for most polymer solutions that obey Cox−Merz rule. However, at low shear rate/angular frequency, the zero shear rate viscosity (η_0) appeared to be in reasonably good agreement. To obtain the zero shear viscosity, the simplified Cross equation was used to fit the complex viscosity curves (Microcal Origin software, version 5.0)

$$\eta = \frac{\eta_0}{1 + (\lambda\dot{\gamma})^{1-n}}$$

where η is the apparent viscosity, η_0 is the zero shear rate viscosity, $\dot{\gamma}$ is the shear rate, λ is the relaxation time, and n is the proportionality constant. The fitting of the Cross equation is somewhat arbitrary, and the values of the three fitting parameters (η_0, λ, and n) depend on initial estimates. The zero-shear viscosity data were used to obtain the concentration dependence of viscosity curve (Figure 6).

The data of the concentration dependence of zero shear rate viscosity plot (Figure 6) for the dilute regime were obtained by viscometric measurements. The data were fitted using the power law equation for the data in dilute and semidilute regimes, respectively. As observed in the graph, the crossover concentration (where the two linear fits intersect) was ~2.2% w/w. In the dilute regime, the exponent value of $\eta_0 \propto c^{1.30}$ is typical of many random coil polymer solutions. However, in the semidilute regime, the exponent value of $\eta_0 \propto c^{4.70}$ is higher than that of entangled random coil polymer ($\sim c^{3.3}$). The higher exponent

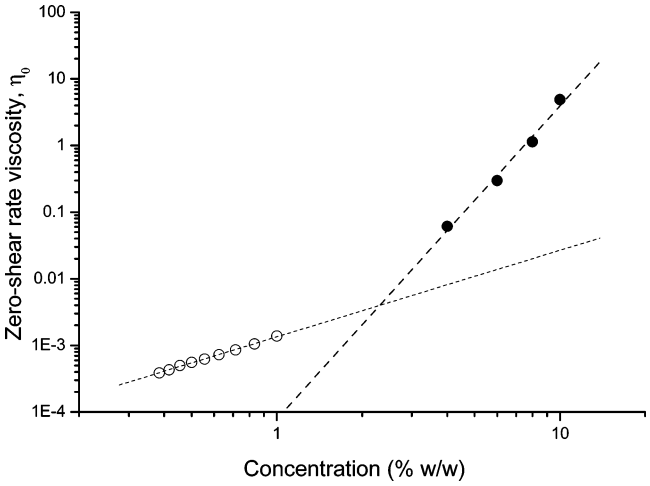

Figure 6. Concentration dependence of zero shear rate viscosity of Mamaku solutions prepared in 0.1 M NaCl and 0.02% sodium azide at 20 °C. Open symbols: zero shear rate specific viscosity data obtained by a Cannon−Ubbelohde low shear four-bulb capillary viscometer (viscometer no. 75, S766, Cannon Instrument Co., U.S.A.). Filled symbols: zero shear rate complex viscosity data estimated by the Cross equation using data from oscillatory measurements.

value in our case could mean that intermolecular interactions among the polymer chains are likely to be present apart from the effect contributed by entanglements of the polymer chain.

3.4. Time-Dependent Shear Measurements. Further experiments were carried out to explore the steady-state of the viscosity data obtained for each shear rate. Viscosity measurements at constant shear rates (0.1, 1, 10, and 100 s^{-1}) were carried out for a period of 1000 s each (Figure 7). At the shear rate of 0.1 s^{-1}, the viscosity decreased slowly with time for the 10% w/w solution. At lower concentrations (8% and 6%), the viscosity curves showed a decreasing trend and then seemed to plateau after ~800 s. At the shear rate of 1 s^{-1}, before the onset of shear-thickening behavior, the viscosity showed an oscillatory pattern across all polymer concentrations used in this study. Such behavior has been reported for steady-state viscosity measure-

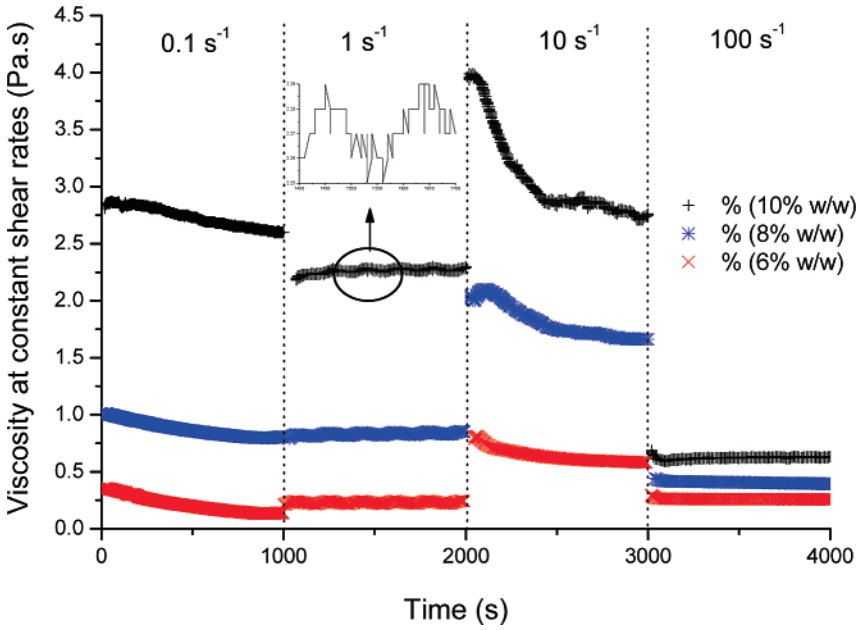

Figure 7. Viscosity of the solutions of Mamaku extract (6%, 8%, and 10% w/w) at 20 °C and at different constant shear rates (0.1, 1, 10, and 100 s^{-1}) each measured over a duration of 1000 s.

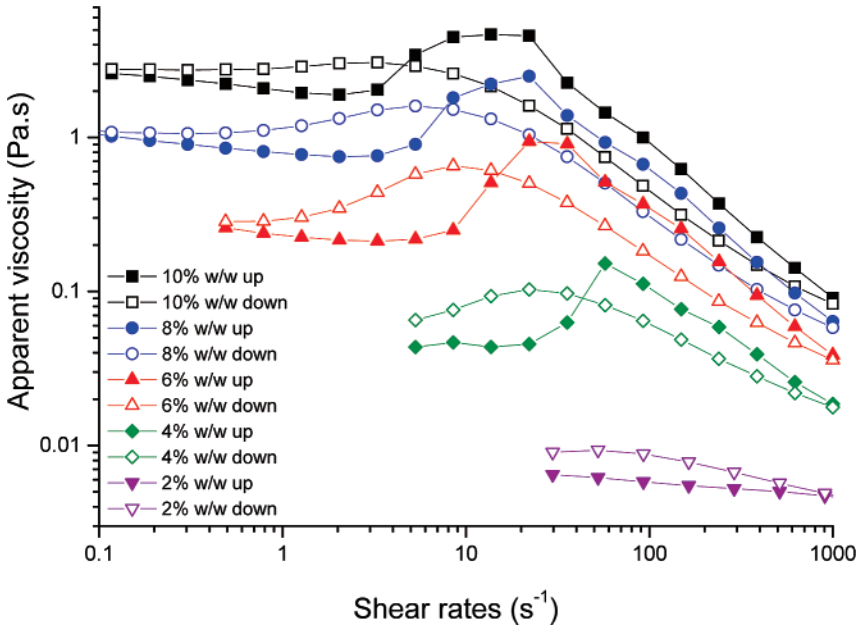

Figure 8. Viscosity curves of the solutions of Mamaku extract (2%, 4%, 6%, 8%, and 10% w/w) as a function of shear rate at 20 °C. Nonlinear viscosity measurements were carried out using double-gap attachment to obtain the "up-curves" (0.1−1000 s^1, filled symbols) and the "down-curves" (1000−0.1 s^{-1}, opened symbols).

ment in the shear-thickening region.[29] In our case, oscillatory pattern occurred before the onset of shear-thickening regime. This behavior could be attributed to an unstable flow (samples are forced out of the gap) at the lower shear rates, implying that a true steady state in the shear rate could not be reached. At 10 s^{-1}, within the shear-thickening regime, the viscosity was the highest at all polymer concentrations with values decreasing over time. Again a steady-state viscosity was not achieved within the experimental time scale. Especially at high concentrations (10% w/w) the big changes in viscosity over time reflects rearrangements of the polymer at the molecular level at this critical shear rate. At 100 s^{-1}, in the shear-thinning regime, steady-state viscosity could be reached within a short period.

Overall, the curves indicate that flow properties of the samples are time-dependent (thixotropic). The complex flow patterns shown by the constant shear rate experiments indicate that the flow behavior of Mamaku solution was different from that of most biopolymers, which are typically entangled random coil polymers. The Mamaku polymer molecules were likely to undergo different conformations and intermolecular interactions at different shear conditions.

To further our understanding of the behavior of the polymer chains during shear, an up−down viscosity sweep (viscosity profile from low to high shear rates and then immediately back from high to low shear rates) was undertaken (Figure 8). The up−down viscosity curves show that Mamaku solution has a wide range of flow behaviors: Newtonian, shear-thickening, shear-thinning, thixotropy, and antithixotropy, depending on the shear conditions. Time-dependent rheological behavior is evident over the entire shear rate range. The occurrences of thixotropic

and antithixotropic behaviors suggest that network disruption and formation, respectively, are present in the system. The up−down viscosity sweep also provides useful information in terms of the rate of network destruction with the application of stress and the network reformation upon the removal of stress. It is important to point out that the viscosity value recorded at the end of a sweep to lower shear rates is the same as the initial viscosity of the system. This indicates that no permanent changes to the chain structure were apparent in the course of performing the up−down sweeps. The extent of thixotropy suggests the slow relaxation of the polymer chains. The relaxation time for the chain to return to its original state when stress was removed seems to be longer than the time of the sweep-down experiment.

3.5. Possible Mechanisms Influencing the Rheological Behaviors. Polymer solutions typically exhibit shear-thinning behavior under the application of shear (viscosity decreases with increasing shear rate). However, Mamaku solutions exhibit anomalous behavior at different shear rates including a shear-thickening regime.

Several theories have been proposed with regard to shear-thickening behavior for associating polymers. Witten and Cohen[30] proposed a mechanism for shear-thickening observed in ionomers in which intermolecular interaction increases during shear at the expense of intramolecular interactions, and eventually there is the formation of a network structure. This theory was further developed quantitatively by Ballard et al.[31] and Vittadello and Biggs.[32]

In the transient network model (TE model) described by Tanaka and Edwards[33] for telechelic polymers, the polymers form a network where the cross-links are small clusters of the functional end groups. However, the shear-thickening behavior was not discussed in the TE model, and moreover, the TE model assumes that topological entanglements are absent. Associative polymers in the entangled semidilute regime are complex, and the dynamics have been described by the concept known as "sticky reptation".[6,34] Based on the concept of the TE model, Wang[35] introduces the idea of chains being elastically effective (forms a network), dangling (one end sticking to junctions), and unbound free chains. It has been proposed that shear-thickening is due to the shear-induced coagulation of free chains to the existing network under moderate shear rates. The junctions formed in the shear-thickening regime are assumed to have a lifetime much longer than the relaxation times of individual chains and network structures. Based on the above models, Marrucci et al.[36] took a different angle by relating shear-thickening to shear-induced chain stretching in the non-Gaussian range of chain behavior. The proportion of intra- and intermolecular associations are assumed to remain constant. Marrucci et al. also reported that fast recapture of dangling ends by the network can produce pronounced shear-thickening. The temporary network structures are continuously disrupted and reformed.[37] Further developments on shear-thickening based on the earlier models have recently been published[9,38,39] and are still a topical subject. Despite the number of models proposed, the molecular origin of shear-thickening has not been completely unravelled.[39]

In our system, we consider that the shear-thickening behavior is generally attributed to shear-induced microstructural changes. Following the assumptions of the TE model,[9,38] the rheological behavior of the Mamaku polymer solution can be qualitatively explained. The Newtonian behavior at the low shear rates could imply compact folded chain structures. Intramolecular interaction dominates within each chain. As shear rate increases, the compact chains start to unfold and elongate. The unfolding of individual chains exposes the functional groups present along the backbone of each chain. This encourages intermolecular interactions to take place which leads to the shear-thickening behavior. The interactions continue to increase to a maximum viscosity at the critical shear rate. Chain stretching in the non-Gaussian range may be present at the same time. Furthermore, the effect of shear-thickening may be contributed by topological entanglements with "sticky" groups present. Beyond the critical shear rate, the applied stress overcomes the intermolecular association. The elongated chains start to break away and align to the direction of the flow. This is where shear-thinning occurs.

From the up−down rotational sweep experiments, the decreasing shear rate during the down sweep allows the elongated chains to reassociate with neighboring chains. Longer time seems to be required for the functional groups to be recaptured by neighboring chains under high shear flow. At intermediate shear rates, the chances of intermolecular interactions are more probable. Here, we observed the antithixotropic behavior. As the shear rates become sufficiently low, intramolecular interactions dominate, eventually causing the elongated molecular chains to return to their folded state at equilibrium under zero-stress condition.

4. Conclusions

This study shows the unique rheological properties of the solution of crude Mamaku extract. At present, the exact mechanism behind the different rheological behaviors at different shear rates has not been unraveled. Further purification of the extracts are necessary to identify the fraction that is responsible for the rheological behaviors. Fundamental studies to characterize the size and conformation of the large molecular weight fraction in dilute solution are underway. In addition, the effects of solvent conditions on the rheological properties are being investigated and will be reported in a forthcoming paper. The unique rheological properties of this material may find many applications such as in coatings, in cosmetics, as food stabilizers/thickeners, as an aid in controlling the flow of food through the digestive tract, and in "smart" fluid systems where viscosity under specific shear rate is required.

Acknowledgment. We thank Dr. Patrick Janssen for introducing the Mamaku frond extract and bringing it to our interest. We also acknowledge the Riddet Centre, Massey University for funding this project.

References and Notes

(1) Crowe, A. *A Field Guide to the Native Edible Plants of New Zealand*, 2nd ed.; Godwit Publishing Limited: Auckland, New Zealand, 1997; pp 107−120.
(2) Brooker, S. G.; Cambie, R. C.; Cooper, R. C. *New Zealand Medicinal Plants*; Reed Publishing (NZ) Ltd: Auckland, New Zealand, 1987; p 72.
(3) Bird, R. B.; Armstrong, R. C.; Hassager, O. *Dynamics of Polymeric Liquids Vol. 1: Fluid Mechanics*; Wiley-Interscience: New York, 1987.
(4) Munoz, M. E.; Santamaria, A. Enhancement of the first normal stress coefficient and dynamic moduli during shear thickening of a polymer solution. *J. Rheol.* **2003**, *47* (4), 1041−1050.
(5) Otsubo, Y. A nonlinear elastic model for shear thickening of suspensions flocculated by reversible bridging. *Langmuir* **1999**, *15* (6), 1960−1965.
(6) van Egmond, J. W. Shear-thickening in suspensions, associating polymers, worm-like micelles, and poor polymer solutions. *Curr. Opin. Colloid Interface Sci.* **1998**, *3* (4), 385−390.
(7) Tam, K. C.; Jenkins, R. D.; Winnik, M. A.; Bassett, D. R. A structural model of hydrophobically modified urethane−ethoxylate (HEUR) associative polymers in shear flows. *Macromolecules* **1998**, *31* (13), 4149−4159.

(8) Ma, S. O. X.; Cooper, S. L. Shear thickening in aqueous solutions of hydrocarbon end-capped poly(ethylene oxide). *Macromolecules* **2001**, *34* (10), 3294−3301.
(9) Koga, T.; Tanaka, F. Molecular origin of shear thickening in transient polymer networks: A molecular dynamics study. *Eur. Phys. J. E* **2005**, *17* (2), 115−118.
(10) Liu, R. C. W.; Morishima, Y.; Winnik, F. M. A rheological evaluation of the interactions in water between a cationic cellulose ether and sodium poly(2-acrylamido-2-methylpropanesulfonates). *Macromolecules* **2001**, *34* (26), 9117−9124.
(11) Chen, X.; Knight, D. P.; Vollrath, F. Rheological characterization of Nephila spidroin solution. *Biomacromolecules* **2002**, *3* (4), 644−648.
(12) Dintzis, F. R.; Bagley, E. B. Shear-thickening and transient flow effects in starch solutions. *J. Appl. Polym. Sci.* **1995**, *56* (5), 637−640.
(13) Kim, S.; Willett, J. L.; Carriere, C. J.; Felker, F. C. Shear-thickening and shear-induced pattern formation in starch solutions. *Carbohydr. Polym.* **2002**, *47* (4), 347−356.
(14) Kjoniksen, A.-L.; Hiorth, M.; Nystrom, B. Association under shear flow in aqueous solutions of pectin. *Eur. Polym. J.* **2005**, *41* (4), 761−770.
(15) Ahn, K. H.; Osaki, K. A network model for predicting the shear thickening behavior of a poly(vinyl alcohol) sodium-borate aqueous-solution. *J. Non-Newtonian Fluid Mech.* **1994**, *55* (3), 215−227.
(16) Dubois, M.; Gilles, J. K.; Hamilton, P. A.; Rebers, P. A.; Smith, F. Colorimetric method for determination of sugars and related substances. *Anal. Chem.* **1956**, *28* (3), 350−356.
(17) Englyst, H. N.; Cummings, J. H. Improved method for measurement of dietary fiber as non-starch polysaccharides in plant foods. *J. Assoc. Off. Anal. Chem.* **1988**, *71* (4), 808−814.
(18) Scott, R. W. Colorimetric determination of hexuronic acids in plant materials. *Anal. Chem.* **1979**, *51* (7), 936−941.
(19) Laun, H. M. Normal stresses in extremely shear thickening polymer dispersions. *J. Non-Newtonian Fluid Mech.* **1994**, *54*, 87−108.
(20) Tuinier, R.; Oomen, C. J.; Zoon, P.; Stuart, M. A. C.; De Kruif, C. G. Viscoelastic properties of an exocellular polysaccharide produced by a *Lactococcus lactis*. *Biomacromolecules* **2000**, *1* (2), 219−223.
(21) Bonn, D.; Kobylko, M.; Bohn, S.; Meunier, J.; Morozov, A.; van Saarloos, W. Rod-climbing effect in Newtonian fluids. *Phys. Rev. Lett.* **2004**, *93* (21), 214503.
(22) Nunez, G. A.; Ribeiro, G. S.; Arney, M. S.; Feng, J.; Joseph, D. D. Rod climbing and normal stresses in heavy crude oils at low shears. *J. Rheol.* **1994**, *38* (5), 1251−1270.
(23) Jomha, A. I.; Reynolds, P. A. An experimental-study of the 1st normal stress difference−shear-stress relationship in simple shear-flow for concentrated shear thickening suspensions. *Rheol. Acta* **1993**, *32* (5), 457−464.
(24) Ma, S. X.; Cooper, S. L. Effect of surfactant on viscoelasticity and shear thickening in aqueous solutions of hydrocarbon end-capped poly(ethylene oxide). *J. Rheol.* **2002**, *46* (2), 339−350.
(25) Martins, A. F.; Leal, C. R.; Godinho, M. H.; Fried, F. The influence of polymer molecular weight on the first normal-stress difference and shear-viscosity of LC solutions of hydroxypropylcellulose. *Mol. Cryst. Liq. Cryst.* **2001**, *362*, 305−312.
(26) Kosvintsev, S. R.; Riande, E.; Velarde, M. G.; Guzman, J. Rheological behaviour of solutions of poly(2-hydroxyethyl methacrylamide) in glycerine. *Polymer* **2001**, *42* (17), 7395−7401.
(27) Lapasin, R.; Pricl, S. *Rheology of Industrial Polysaccharides: Theory and Applications*; Blackie Academic and Professional: Great Britain, 1995.
(28) Cox, W. P.; Merz, E. H. Correlation of dynamic and steady flow viscosities. *J. Polym. Sci.* **1958**, *28*, 619−622.
(29) Hilliou, L.; Vlassopoulos, D. Time-periodic structures and instabilities in shear-thickening polymer solutions. *Ind. Eng. Chem. Res.* **2002**, *41* (25), 6246−6255.
(30) Witten, T. A.; Cohen, M. H. Cross-linking in shear-thickening ionomers. *Macromolecules* **1985**, *18* (10), 1915−1918.
(31) Ballard, M. J.; Buscall, R.; Waite, F. A. The theory of shear-thickening polymer-solutions. *Polymer* **1988**, *29* (7), 1287−1293.
(32) Vittadello, S. T.; Biggs, S. Shear history effects in associative thickener solutions. *Macromolecules* **1998**, *31* (22), 7691−7697.
(33) Tanaka, F.; Edwards, S. F. Viscoelastic properties of physically cross-linked networks. 1. Transient network theory. *Macromolecules* **1992**, *25* (5), 1516−1523.
(34) Leibler, L.; Rubinstein, M.; Colby, R. H. Dynamics of reversible networks. *Macromolecules* **1991**, *24* (16), 4701−4707.
(35) Wang, S. Q. Transient network theory for shear-thickening fluids and physically cross-linked systems. *Macromolecules* **1992**, *25* (25), 7003−7010.
(36) Marrucci, G.; Bhargava, S.; Cooper, S. L. Models of shear-thickening behavior in physically cross-linked networks. *Macromolecules* **1993**, *26* (24), 6483−6488.
(37) Vaccaro, A.; Marrucci, G. A model for the nonlinear rheology of associating polymers. *J. Non-Newtonian Fluid Mech.* **2000**, *92* (2−3), 261−273.
(38) Tanaka, F.; Koga, T. Nonaffine transient network theory of associating polymer solutions. *Macromolecules* **2006**, *39* (17), 5913−5920.
(39) Indei, T.; Koga, T.; Tanaka, F. Theory of shear-thickening in transient networks of associating polymer. *Macromol. Rapid Commun.* **2005**, *26* (9), 701−706.

BM7005328